



Contents lists available at ScienceDirect

Polyhedron

journal homepage: [www.elsevier.com/locate/poly](http://www.elsevier.com/locate/poly)

# Effect of ancillary (aminomethyl)phenolate ligand on efficacy of aluminum-catalyzed glucose dehydration to 5-hydroxymethylfurfural

Daudi Saang'onyo, Sean Parkin, Folami T. Ladipo\*

Chemistry Department, University of Kentucky, Lexington, KY 40506-0055, USA



## ARTICLE INFO

### Article history:

Received 29 December 2017

Accepted 30 March 2018

Available online 4 May 2018

### Keywords:

Glucose

5-Hydroxymethylfurfural

Aluminum catalysts

Dehydration

Ionic liquids

## ABSTRACT

Air-stable dimethylaluminum complexes  $L^RAlMe_2$  that contain (aminomethyl)phenolate ( $L^R$ ) were prepared in high yield. NMR data and X-ray crystallographic characterization of the structures of several of the complexes confirmed bidentate coordination of the (aminomethyl)phenolate ligand to aluminum. Efficient aluminum catalysts for glucose dehydration to HMF were generated by modification of the (aminomethyl)phenolate ligand.  $L^RAlMe_2$  complexes containing bidentate (aminomethyl)phenolate ligands with an aryl substituent on the amino moiety are efficient catalysts for glucose dehydration to HMF in ionic liquid solvents. In [EMIM]Br and [BMIM]Br, the reaction proceeds at room temperature to very high conversion in 2 h to produce HMF with 60–63% selectivity and in 58–60% yield. Even in the absence of ionic liquid,  $L^RAlMe_2$  complexes catalyze glucose isomerization to fructose at  $\geq 120$  °C while the HMF yield is dependent on the degree of competing HMF loss to humins formation. These results indicate that additional ancillary ligand effects on aluminum-catalyzed glucose dehydration are needed to improve knowledge of structure–function relationships that are key to increasing the efficiency of aluminum-catalyzed dehydration of glucose (and ultimately cellulose) to HMF.

Published by Elsevier

## 1. Introduction

Glucose is the most abundant monosaccharide in cellulosic biomass hence efficient catalytic processes for its conversion into chemicals and biofuels are highly desirable [1–3]. Glucose dehydration is a promising method for synthesis of 5-hydroxymethylfurfural (HMF), an emerging bio-derived platform chemical that potentially could be used to produce a wide variety of high-value chemicals [4,5]. For example, HMF can be converted by selective oxidation into 2,5-furandicarboxylic acid (FDCA) which is attractive as a substitute for terephthalic acid in plastics production [6,7]. HMF can also undergo rehydration to produce levulinic acid (LA) which itself is a promising platform chemical that can be used as a feedstock for production of liquid hydrocarbon fuels [8,9].

give HMF in low yield and produce other byproducts, moderate to-high yields of HMF have been reported in ionic liquids and boiling organic solvents with various Lewis acid metal salts such as  $CrCl_2$  [11–13],  $SnCl_4$  [14,15], and  $AlCl_3$  [10,16–18] as catalysts.

Given the much lower toxicity and cheaper cost of Al in comparison to Cr and Sn, the development of efficient Al catalysts for glucose conversion to HMF is receiving increased attention [19,20]. For example, Abu-Omar and coworkers have reported that  $AlCl_3$  exhibits high glucose conversion activity in water/THF biphasic medium to give HMF in 61% yield [16]. Dumesic and coworkers found that catalytic conversion of glucose with the combination of  $AlCl_3$  and a Brønsted acid (such as HCl) in a biphasic water/alkanol solvent system gave 62% yield of HMF [10]. Rasrendra et al. reported that both  $AlCl_3$  and  $Al(OTf)_3$  in DMSO for glucose conversion to p

Investigations of glucose dehydration [5] using different catalysts (such as organic and inorganic acids, Lewis acids, salts, and zeolites) and solvents (including aqueous, organic, mixed aqueous/organic, and ionic liquids) have established that glucose conversion to HMF with Brønsted acids (such as HCl and H<sub>2</sub>SO<sub>4</sub>) typically proceeds via direct dehydration of glucose to HMF while with Lewis acid catalysts, the reaction typically proceeds via formation of fructose [6,10]. However, while mineral acids usually

\* Corresponding author.

HMF in 50% and 60% yield, respectively [19]. Liu and Chen showed that aluminum trialkyls (such as pyrophoric AlMe<sub>3</sub> and AlEt<sub>3</sub>) and trialkoxides (such as Al(OPr<sup>i</sup>)<sub>3</sub> and Al(OBu<sup>t</sup>)<sub>3</sub>) can give up to 100% HMF yield from glucose conversion in [EMIM]Cl [20]. These studies indicate that aluminum species hold strong promise as Lewis acid catalysts for glucose conversion to HMF. However, the majority of studies used (10–30%) AlCl<sub>3</sub> in different solvents, and current knowledge of ancillary ligand effects on the efficiency of glucose conversion to HMF with aluminum Lewis acid catalysts is lacking. Herein, we report a systematic study of the efficacy of easily prepared air-stable dimethylaluminum complexes containing bidentate

(aminomethyl)phenolate ligands as catalysts for the conversion of glucose to HMF in ionic liquids. We demonstrate that effective catalysts for glucose dehydration to HMF can be produced via modification of the (aminomethyl)phenolate ligand.

## 2. Experimental

### 2.1. General comments

All manipulations of air- and/or moisture-sensitive compounds were carried out under dry nitrogen atmosphere using standard Schlenk or glovebox techniques. All solvents were dried and distilled by standard methods [21] prior to use and stored in a glovebox over 4A molecular sieves that had been dried in a vacuum oven at 150 °C for at least 48 h. All other chemicals were used as received, unless otherwise stated. Toluene, THF, ethanol, petroleum ether, *n*-hexane, chloroform, methylene chloride, and methanol (all ACS grade) were purchased from Pharmco-Aaper. Ethyl acetate and acetonitrile were purchased from Fisher Scientific. 5-Hydroxymethylfurfural (~99%), D-(–)-fructose, D-(+)-glucose (≥99.5%), AlMe<sub>3</sub> (2.0 M in hexane), 2-*tert*-butyl-4-methylphenol (99%), *N*-methylbenzylamino (97%), *N*-ethylbenzylamino (97%), *N*-isopropylbenzylamine (97%), *N*-phenylaniline (99%), 4-methylaniline (99.6%), 4-chloroaniline (98%), benzaldehyde (≥98%) and poly(methylhydrosiloxane) were purchased from Sigma–Aldrich. Paraformaldehyde (96%), 1-ethyl-3-methylimidazolium chloride ([EMIM]Cl, 97%), and 1-ethyl-3-methylimidazolium bromide ([EMIM]Br, 97%) were purchased from Acros Organics. [EMIM]Cl and [EMIM]Br were purified before use, via recrystallization according to the literature method [22]. [BMIM]Br was synthesized and purified by following literature methods [22,23]. *N*-(*tert*-Butyl)benzylamino (99%) was purchased from Alfa Aesar. *N*-benzyl-4-chloroaniline [24], *N*-benzyl-*p*-toluidine [24], 2-[(*N*-benzyl-*N*-methyl)aminomethyl]-6-*tert*-butyl-4-methylphenol (**1a**) [25], 2-[(*N*-benzyl-*N*-ethyl-aminomethyl)-4-methyl-6-*tert*-butyl-phenol (**1b**) [26], and L<sup>Et</sup>AlMe<sub>2</sub> (**2b**, L<sup>Et</sup> = 2-[(*N*-benzyl-*N*-ethyl-aminomethyl)-4-methyl-6-*tert*-butyl-phenolate) [26] were prepared by the literature methods or modification thereof.

<sup>1</sup>H and <sup>13</sup>C{<sup>1</sup>H} NMR spectra were recorded on a Varian VXR-400 spectrometer at room temperature. All chemical shifts are reported in units of δ (downfield from tetramethylsilane) and were referenced to residual solvent peaks. FTIR spectra were collected

29.97 mmol) were charged into a heavy-walled reaction vessel equipped with a magnetic stir bar. The vessel was capped tightly and then placed in an oil bath maintained at 105 °C, and heated with stirring for 1 h. After cooling to room temperature, the light-yellow reaction mixture was dissolved in chloroform (50 mL). The solution was washed with distilled water (5 × 15 mL) and dried over anhydrous Na<sub>2</sub>SO<sub>4</sub> for 12 h. After filtering off Na<sub>2</sub>SO<sub>4</sub>, the filtrate was evaporated under reduced pressure to give a pale-yellow oil, which was purified by silica gel column chromatography using 20:1 petroleum ether:ethyl acetate as eluent. The solution was evaporated under reduced pressure to give **1c** as a colorless oil. The material was collected and dried under reduced pressure. Yield: 5.4 g, 82.9%. <sup>1</sup>H NMR (400 MHz, CDCl<sub>3</sub>): δ 11.15 (br s, 1H, OH), 7.15 (m, 5H, ArH), 6.92 (d, <sup>4</sup>J = 2.0 Hz, 1H, ArH), 6.64 (d, <sup>4</sup>J = 2.0 Hz, 1H, ArH), 3.67 (s, 2H, ArCH<sub>2</sub>), 3.51 (s, 2H, PhCH<sub>2</sub>), 2.99 (s, 1H, <sup>3</sup>J = 7.2 Hz, CH(CH<sub>3</sub>)<sub>2</sub>), 2.18 (s, 3H, ArCH<sub>3</sub>), 1.37 (s, 9H, (CH<sub>3</sub>)<sub>3</sub>), 1.06 (d, 6H, <sup>3</sup>J = 7.2 Hz, NCH(CH<sub>3</sub>)<sub>2</sub>). <sup>13</sup>C{H} NMR (100 MHz, CDCl<sub>3</sub>): δ 154.7, 138.5, 136.4, 129.6, 128.7, 127.8, 127.1, 126.6, 122.4 (all Ar–C), 54.0 (ArCH<sub>2</sub>), 52.7 (PhCH<sub>2</sub>), 34.8 (C(CH<sub>3</sub>)<sub>3</sub>), 29.7 (ArC(CH<sub>3</sub>)<sub>3</sub>), 21.0 (ArCH<sub>3</sub>), 1.06 (NCH(CH<sub>3</sub>)<sub>2</sub>).

### 2.2.2. Synthesis of 2-[(*N*-benzyl-*N*-*tert*-butyl)aminomethyl]-6-*tert*-butyl-4-methylphenol (**1d**)

This compound was prepared following a similar procedure to that described for **1c**, from 2-*tert*-Butyl-4-methylphenol (3.27 g, 19.98 mmol), *N*-*tert*-butylbenzylamine (3.27 g, 20.04 mmol) and paraformaldehyde (0.60 g, 19.98 mmol). After purification of the reaction product, a light-yellow oil, by silica gel column chromatography (using 20:1 petroleum ether:ethyl acetate as eluent) and removal of the organic volatiles under reduced pressure furnished a light-yellow oil that was recrystallized from hexane at –20 °C, giving **1d** as white crystals. The material was collected and dried under reduced pressure. Yield: 4.46 g, 65.7%. <sup>1</sup>H NMR (400 MHz, CDCl<sub>3</sub>): δ 10.98 (s, 1H, OH), 7.23–7.06 (m, 5H, ArH), 6.88 (d, <sup>4</sup>J = 1.6 Hz, 1H, ArH), 6.61 (d, <sup>4</sup>J = 1.6 Hz, 1H, ArH), 3.84 (s, 2H, ArCH<sub>2</sub>), 3.70 (s, 2H, PhCH<sub>2</sub>), 2.19 (s, 3H, ArCH<sub>3</sub>), 1.37 (s, 9H, NC(CH<sub>3</sub>)<sub>3</sub>), 1.21 (s, 9H, ArC(CH<sub>3</sub>)<sub>3</sub>). <sup>13</sup>C{H} NMR (100 MHz, CDCl<sub>3</sub>): δ 140.9, 136.4, 128.9, 128.3, 127.2, 127.1, 126.8, 126.3, 124.0 (all Ar–C), 57.1 (NC(CH<sub>3</sub>)<sub>3</sub>), 54.6 (ArCH<sub>2</sub>), 54.4 (PhCH<sub>2</sub>), 34.7 (C(CH<sub>3</sub>)<sub>3</sub>), 29.7 (NC(CH<sub>3</sub>)<sub>3</sub>), 27.2 (ArC(CH<sub>3</sub>)<sub>3</sub>), 21.0 (ArCH<sub>3</sub>).

on a Thermo Scientific Nicolet 6700 ATR-FTIR spectrometer fitted with a ZnSe crystal with a Smart iTR accessory. The resolution of the instrument was set to  $4\text{ cm}^{-1}$ . The background of the IR spectrum of air was first collected, and then powdered samples were placed on the ZnSe crystal, pressed against the crystal using the inbuilt high-pressure clamp and their absorbance was measured. A total of 40 s scans were used for both background and the samples. Raman spectra were collected on a DXR Raman microscope (Thermo Fisher) spectrometer. The source of radiation was a laser operated at 532 nm. The excitation laser beam was focused on the sample using a microscope equipped with a  $10\times$  lens. The laser power at the sample surface was about 2 mW and the acquisition time for each spectrum was 20 s and recorded in the range of  $50\text{--}3500\text{ cm}^{-1}$ . X-ray diffraction data were collected at  $90.0(2)\text{ K}$  on either a Nonius kappaCCD, Bruker-Nonius X8 Proteum, or a D8 Venture diffractometer. Elemental analysis for C, H, and N was performed by Robertson Microlit Laboratories, Ledgewood, NJ.

## 2.2. Synthesis of the proligands

ture was heated for 6 h. After purification by silica gel column chromatography using 5:1 hexane:ethyl acetate as eluent, **1f** was obtained as a white powder. Yield: 1.63 g, 50.4%.  $^1\text{H NMR}$  (400 MHz,  $\text{CDCl}_3$ ):  $\delta$  9.99 (s, 1H, OH), 7.22–7.18 (m, 3H, ArH), 7.06–6.95 (m, 7H, ArH), 6.72 (d,  $^4J = 1.6\text{ Hz}$ , 1H, ArH), 4.23 (s, 2H,  $\text{ArCH}_2$ ), 4.17 (s, 2H,  $\text{ArCH}_2$ ), 2.27 (s, 3H,  $\text{NArCH}_3$ ), 2.25 (s, 3H,  $\text{ArCH}_3$ ), 1.42 (s, 9H,  $\text{C}(\text{CH}_3)_3$ ).  $^{13}\text{C}\{\text{H}\}$  NMR (100 MHz,  $\text{CDCl}_3$ ):  $\delta$  154.4, 146.8, 136.7, 136.5, 133.6, 129.9, 129.6, 128.4, 127.9, 127.7, 127.5, 127.1, 122.5, 122.2 (all Ar–C), 58.1 ( $\text{ArCH}_2$ ), 57.7 ( $\text{PhCH}_2$ ), 34.8 ( $\text{C}(\text{CH}_3)_3$ ), 29.8 ( $\text{C}(\text{CH}_3)_3$ ), 21.1 ( $\text{NArCH}_3$ ), 21.0 ( $\text{ArCH}_3$ ).

### 2.2.5. Synthesis of 2-[(*N*-benzyl-*N*-(*p*-chlorophenyl))aminomethyl]-6-*tert*-butyl-4-methylphenol (**1g**)

This compound was prepared following a similar procedure to that described for **1c**, from 2-*tert*-butyl-4-methylphenol (0.37 g, 2.25 mmol), paraformaldehyde (0.10 g, 3.38 mmol), and *N*-benzyl-4-chloroaniline [24] (0.49 g, 2.25 mmol), except the reaction mixture was heated for 50 h. After purification by silica gel column chromatography using 20:1 petroleum ether:ethyl acetate as eluent, **1g** was obtained as a white powder. Yield: 0.66 g, 73.9%.  $^1\text{H NMR}$  (400 MHz,  $\text{CDCl}_3$ ):  $\delta$  9.26 (s, 1H, OH), 7.23–7.17 (m, 5H, ArH), 7.03–6.96 (m, 5H, ArH), 6.70 (d, 1H,  $^4J = 1.6\text{ Hz}$ , ArH), 4.23 (s, 2H,  $\text{ArCH}_2$ ), 4.22 (s, 2H,  $\text{ArCH}_2$ ), 2.24 (s, 3H,  $\text{ArCH}_3$ ), 1.40 (s, 9H,  $\text{C}(\text{CH}_3)_3$ ).  $^{13}\text{C}\{\text{H}\}$  NMR (100 MHz,  $\text{CDCl}_3$ ):  $\delta$  154.0, 147.9, 136.9, 136.0, 129.4, 129.3, 128.6, 128.1, 127.9, 127.8, 127.4, 123.2, 121.8 (all Ar–C), 57.8 ( $\text{ArCH}_2$ ), 56.8 ( $\text{ArCH}_2$ ), 34.8 ( $\text{C}(\text{CH}_3)_3$ ), 29.8 ( $\text{C}(\text{CH}_3)_3$ ), 21.1 ( $\text{ArCH}_3$ ).

## 2.3. Synthesis of aluminum complexes

### 2.3.1. Synthesis of $L^{\text{Me}}\text{AlMe}_2$ complex (**2a**)

$\text{AlMe}_3$  (4.50 mL, 8.97 mmol, 2.0 M in hexane) was added dropwise to a toluene (20 mL) solution of 2-[(*N*-benzyl-*N*-methyl)aminomethyl]-6-*t*-butyl-4-methylphenol [25] (**1a**, 2.67 g, 8.97 mmol) at room temperature. Evolution of methane was immediately observed. The reaction mixture was stirred for 24 h at room temperature. All of the volatiles were removed under reduced pressure to give a foam-like white solid, which was dissolved in *n*-hexane

### 2.2.3. Synthesis of 2-[(*N*-benzyl-*N*-phenyl)aminomethyl]-6-*tert*-butyl-4-methylphenol (**1e**)

This compound was prepared following a similar procedure that described for **1c**, from 2-*tert*-butyl-4-methylphenol (3.2 g, 19.98 mmol), paraformaldehyde (0.60 g, 19.98 mmol), and phenylbenzylamine (3.67 g, 20.04 mmol). After purification of the reaction product, a light-yellow oil, by silica gel column chromatography (using 5:1 hexane:ethyl acetate as eluent), removal of the organic volatiles under reduced pressure gave **1e** as white crystals. Yield: 4.53 g, 63.1%.  $^1\text{H NMR}$  (400 MHz,  $\text{CDCl}_3$ ):  $\delta$  9.99 (br s, 1H, OH), 7.28–7.16 (m, 5H, ArH), 7.10–6.96 (m, 6H, ArH), 6.71 (d,  $^4J = 1.6\text{ Hz}$ , 1H, ArH), 4.26 (s, 2H,  $\text{ArCH}_2$ ), 4.22 (s, 2H,  $\text{ArCH}_2$ ), 2.24 (s, 3H,  $\text{ArCH}_3$ ), 1.41 (s, 9H,  $\text{C}(\text{CH}_3)_3$ ).  $^{13}\text{C}\{\text{H}\}$  NMR (100 MHz,  $\text{CDCl}_3$ ):  $\delta$  154.2, 149.4, 136.8, 136.3, 129.4, 128.4, 128.0, 127.9, 127.6, 127.2, 123.7, 122.1, 122.0 (all Ar–C), 57.6 ( $\text{ArCH}_2$ ), 57.0 ( $\text{PhCH}_2$ ), 34.8 ( $\text{C}(\text{CH}_3)_3$ ), 29.8 ( $\text{C}(\text{CH}_3)_3$ ), 21.1 ( $\text{ArCH}_3$ ).

### 2.2.4. Synthesis of 2-[(*N*-benzyl-*N*-*p*-toluidine)aminomethyl]-6-*tert*-butyl-4-methylphenol (**1f**)

3.92 (d,  $^2J = 13.2\text{ Hz}$ , 1H,  $\text{ArCH}_2$ ), 3.89 (d,  $^2J = 13.2\text{ Hz}$ , 1H,  $\text{ArCH}_2$ ), 3.55 (d,  $^2J = 13.2\text{ Hz}$ , 1H,  $\text{ArCH}_2$ ), 2.24 (s, 3H,  $\text{NCH}_3$ ), 2.22 (s, 3H,  $\text{ArCH}_3$ ), 1.39 (s, 9H,  $\text{C}(\text{CH}_3)_3$ ),  $-0.62$  (s, 3H,  $\text{AlCH}_3$ ),  $-0.86$  (s, 3H,  $\text{AlCH}_3$ ).  $^{13}\text{C}\{\text{H}\}$  NMR (100 MHz,  $\text{CDCl}_3$ ):  $\delta$  156.7, 138.9, 129.8, 129.4, 128.8, 128.5, 128.2, 125.1, 120.4 (all Ar–C), 59.0 ( $\text{PhCH}_2$ ), 40.2 ( $\text{NCH}_3$ ), 35.0 ( $\text{C}(\text{CH}_3)_3$ ), 29.7 ( $\text{C}(\text{CH}_3)_3$ ), 20.9 ( $\text{ArCH}_3$ ),  $-10.3$  ( $\text{AlCH}_3$ ),  $-10.9$  ( $\text{AlCH}_3$ ). *Anal. Calc.* for  $\text{C}_{24}\text{H}_{36}\text{AlNO}$ : C, 74.75; H, 9.12; N, 3.96. Found: C, 74.80; H, 9.54; N, 3.96.

### 2.3.2. Synthesis of $L^{\text{i-Pr}}\text{AlMe}_2$ complex (**2c**)

Complex **2c** was obtained as a white powder, by following a similar procedure to that described for **2a**, from reaction between  $\text{AlMe}_3$  (1.40 mL, 2.87 mmol, 2.0 M in hexane) and **1c** (0.37 g, 2.87 mmol). Yield: 0.92 g, 83.9%.  $^1\text{H NMR}$  (400 MHz,  $\text{CDCl}_3$ ):  $\delta$  7.37–7.21 (m, 5H, ArH), 7.03 (d,  $^4J = 2.0\text{ Hz}$ , 1H, ArH), 6.68 (d,  $^4J = 2.0\text{ Hz}$ , 1H, ArH), 4.23 (d,  $^2J = 14.0$ , 1H,  $\text{ArCH}_2$ ), 4.16 (d,  $^2J = 14.0$ , 1H,  $\text{ArCH}_2$ ), 3.95 (d,  $^2J = 14.0\text{ Hz}$ , 1H,  $\text{ArCH}_2$ ), 3.59 (d,  $^2J = 14.0$ , 1H,  $\text{ArCH}_2$ ), 3.17 (sept., 1H,  $^3J = 6.8\text{ Hz}$ ,  $\text{CH}(\text{CH}_3)_2$ ), 2.27 (s, 3H,  $\text{ArCH}_3$ ), 1.38 (s, 9H,  $\text{C}(\text{CH}_3)_3$ ), 1.36 (d, 3H,  $^3J = 7.2\text{ Hz}$ ,  $\text{CH}(\text{CH}_3)_2$ ), 1.25 (d, 3H,  $^3J = 6.8\text{ Hz}$ ,  $\text{CH}(\text{CH}_3)_2$ ),  $-0.64$  ( $\text{AlCH}_3$ ),  $-0.68$  ( $\text{AlCH}_3$ ).  $^{13}\text{C}\{\text{H}\}$  NMR (100 MHz,  $\text{CDCl}_3$ ):  $\delta$  156.6, 139.0, 132.2, 129.0, 128.7, 128.6, 128.1, 125.3, 120.8 (all Ar–C), 55.4 ( $\text{ArCH}_2$ ), 53.8 ( $\text{ArCH}_2$ ), 52.2 ( $\text{CH}(\text{CH}_3)_2$ ), 35.0 ( $\text{C}(\text{CH}_3)_3$ ), 29.7 ( $\text{C}(\text{CH}_3)_3$ ), 19.4 ( $\text{CH}(\text{CH}_3)_2$ ), 19.1 ( $\text{CH}(\text{CH}_3)_2$ ),  $-7.1$  ( $\text{AlCH}_3$ ),  $-7.1$  ( $\text{AlCH}_3$ ). *Anal. Calc.* for  $\text{C}_{24}\text{H}_{36}\text{AlNO}$ : C, 75.55; H, 9.51; N, 3.96. Found: C, 74.50; H, 9.48; N, 3.64%.

### 2.3.3. Synthesis of $L^{\text{t-Bu}}\text{AlMe}_2$ complex (**2d**)

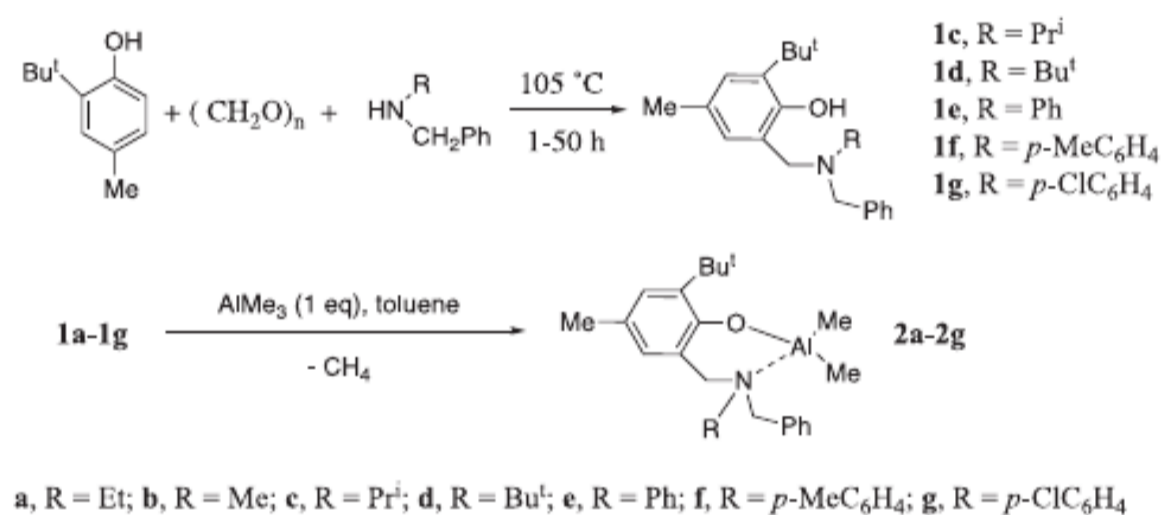
Complex **2d** was obtained as a light-yellow powder, by following a similar procedure to that described for **2a**, from reaction between  $\text{AlMe}_3$  (1.0 mL, 2.00 mmol, 2.0 M in hexane) and **1a** (0.79 g, 2.00 mmol). Yield: 0.637 g, 80.5%.  $^1\text{H NMR}$  (400 MHz,  $\text{CDCl}_3$ ):  $\delta$  7.37–7.31 (m, 2H, ArH), 7.30–7.25 (m, 3H, ArH), 7.25 (d,  $^4J = 2.0\text{ Hz}$ , 1H, ArH), 6.72 (d,  $^4J = 2.0\text{ Hz}$ , 1H, ArH), 4.47 (d,  $^2J = 15.2$ , 1H,  $\text{ArCH}_2$ ), 4.36 (d,  $^2J = 15.2\text{ Hz}$ , 1H,  $\text{ArCH}_2$ ), 4.26 (d,  $^2J = 15.2\text{ Hz}$ , 1H,  $\text{ArCH}_2$ ), 4.11 (d,  $^2J = 14.8\text{ Hz}$ , 1H,  $\text{ArCH}_2$ ), 2.26 (s, 3H,  $\text{ArCH}_3$ ), 1.37 (s, 9H,  $\text{NC}(\text{CH}_3)_3$ ), 1.26 (s, 9H,  $\text{ArC}(\text{CH}_3)_3$ ),

and filtered to remove trace impurities. The filtrate was concentrated and kept at  $-20^{\circ}\text{C}$  overnight. Subsequently, **2a** was collected as a white precipitate and dried under reduced pressure. Yield: 2.32 g, 73.3%.  $^1\text{H}$  NMR (400 MHz,  $\text{CDCl}_3$ ):  $\delta$  7.44–7.37 (m, 3H, ArH), 7.33–7.27 (m, 2H, ArH), 7.04 (d, 1H,  $^4J = 2.0$  Hz, ArH), 6.56 (d,  $^4J = 2.0$  Hz, 1H, ArH), 3.97 (d,  $^2J = 13.2$  Hz, 1H, ArCH<sub>2</sub>),

(AlCH<sub>3</sub>),  $-0.63$  (AlCH<sub>3</sub>).  $^{13}\text{C}\{\text{H}\}$  NMR (100 MHz,  $\text{CDCl}_3$ ):  $\delta$  139.4, 135.1, 131.8, 128.8, 128.5, 128.1, 127.6, 125.4, 121.1 (Ar–C), 62.4 (NC(CH<sub>3</sub>)<sub>3</sub>), 52.6 (ArCH<sub>2</sub>), 52.3 (PhCH<sub>2</sub>) (CH<sub>3</sub>)<sub>3</sub>, 29.6 (NC(CH<sub>3</sub>)<sub>3</sub>), 28.2 (ArC(CH<sub>3</sub>)<sub>3</sub>), 21.1 (ArCH<sub>3</sub>) (AlCH<sub>3</sub>),  $-7.3$  (AlCH<sub>3</sub>). Anal. Calc. for C<sub>25</sub>H<sub>38</sub>AlNO: C, 75.96%; H, 9.68%; N, 3.54. Found: C, 75.31%; H, 9.97%; N, 3.51%.

**Table 1**  
Crystallographic Data for L<sup>R</sup>AlMe<sub>2</sub> complexes **2a–c**, **2e**, and **2f**.

Complex	<b>2a</b>	<b>2b</b>	<b>2c</b>	<b>2e</b>	<b>2f</b>
Formula	C <sub>22</sub> H <sub>32</sub> AlNO	C <sub>23</sub> H <sub>34</sub> AlNO	C <sub>24</sub> H <sub>36</sub> AlNO	C <sub>27</sub> H <sub>34</sub> AlNO	C <sub>28</sub> H <sub>36</sub> AlNO
Formula weight	353.46	367.49	381.52	415.53	429.56
T (K)	90.0(2)	90.0(2)	90.0(2)	90.0(2)	90.0(2)
Crystal system	monoclinic	monoclinic	monoclinic	monoclinic	monoclinic
Space group	P2(1)/n	P2(1)/n	P2(1)/n	P2(1)/c	P2(1)/c
Unit cell dimensions					
a (Å)	9.6557(2)	11.1393(4)	11.5303(4)	12.0981(2)	9.2418(3)
b (Å)	12.6012(2)	9.6143(3)	18.1337(7)	17.9578(4)	21.7215(6)
c (Å)	17.5369(3)	20.1941(8)	12.0678(5)	12.0051(2)	12.4113(3)
$\alpha$ (°)	90	90	90	90	90
$\beta$ (°)	99.0269(8)	91.854(3)	117.291(2)	116.0401(12)	98.493(1)
$\gamma$ (°)	90	90	90	90	90
V (Å <sup>3</sup> )	2107.35(7)	2161.59(13)	2242.36(15)	2343.41(8)	2464.19(10)
Z	4	4	4	4	4
D <sub>calc.</sub> (g/cm <sup>3</sup> )	1.114	1.129	1.130	1.178	1.158
Final R indices [I > 2 $\sigma$ (I)]	0.0445 0.1178	0.0548 0.1458	0.0336 0.0857	0.0430 0.1053	0.0344 0.1053



**Scheme 1.** Synthesis of proligands **1c–g** and L<sup>R</sup>AlMe<sub>2</sub> complexes **2a–g**.

### 2.3.4. Synthesis of L<sup>Ph</sup>AlMe<sub>2</sub> complex (**2e**)

Complex **2e** was obtained as a white powder, by following a similar procedure to that described for **2a**, from reaction between AlMe<sub>3</sub> (1.74 mL, 3.48 mmol, 2.0 M in hexane) and **1e** (1.25 g, 3.48 mmol). Yield: 1.16 g, 79.9%.  $^1\text{H}$  NMR (400 MHz,  $\text{CDCl}_3$ ):  $\delta$  7.48–7.36 (m, 4H, ArH), 7.35–7.29 (m, 1H, ArH), 7.25–7.19 (m, 1H, ArH), 7.13–7.04 (m, 3H, ArH), 6.59–6.52 (m, 3H, ArH), 4.57 (d,  $^2J = 14.0$  Hz, 1H, ArCH<sub>2</sub>), 4.43 (d,  $^2J = 12.8$  Hz, 1H, ArCH<sub>2</sub>), 4.20 (d,  $^2J = 14.0$  Hz, 1H, ArCH<sub>2</sub>), 3.81 (d,  $^2J = 12.8$  Hz, 1H, ArCH<sub>2</sub>), 2.28 (s, 3H, ArCH<sub>3</sub>), 1.44 (s, 9H, C(CH<sub>3</sub>)<sub>3</sub>),  $-0.43$  (AlCH<sub>3</sub>),  $-1.26$  (AlCH<sub>3</sub>).  $^{13}\text{C}\{\text{H}\}$  NMR (100 MHz,  $\text{CDCl}_3$ ):  $\delta$  157.0, 145.8, 138.9, 131.5, 130.8, 129.9, 129.8, 129.0, 128.5, 128.0, 127.0, 125.0, 122.4, 119.5 (all Ar–C), 58.5 (ArCH<sub>2</sub>), 53.3 (PhCH<sub>2</sub>), 35.0 (C(CH<sub>3</sub>)<sub>3</sub>), 29.7 (C(CH<sub>3</sub>)<sub>3</sub>), 21.0 (ArCH<sub>3</sub>),  $-9.5$  (AlCH<sub>3</sub>),  $-10.4$  (AlCH<sub>3</sub>). Anal. Calc. for C<sub>27</sub>H<sub>34</sub>AlNO: C, 78.04%; H, 8.23%; N, 3.37. Found: C, 78.50%; H, 8.71%; N, 3.38%.

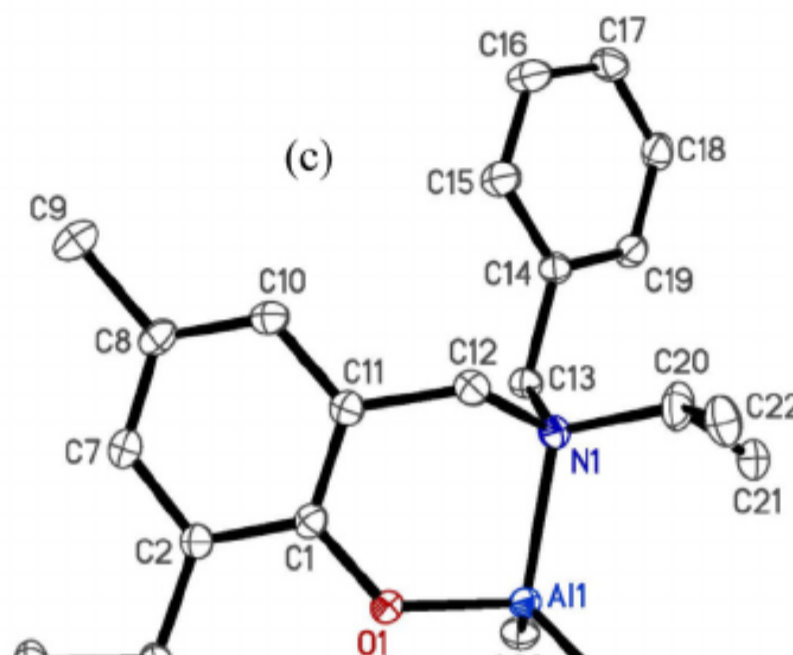
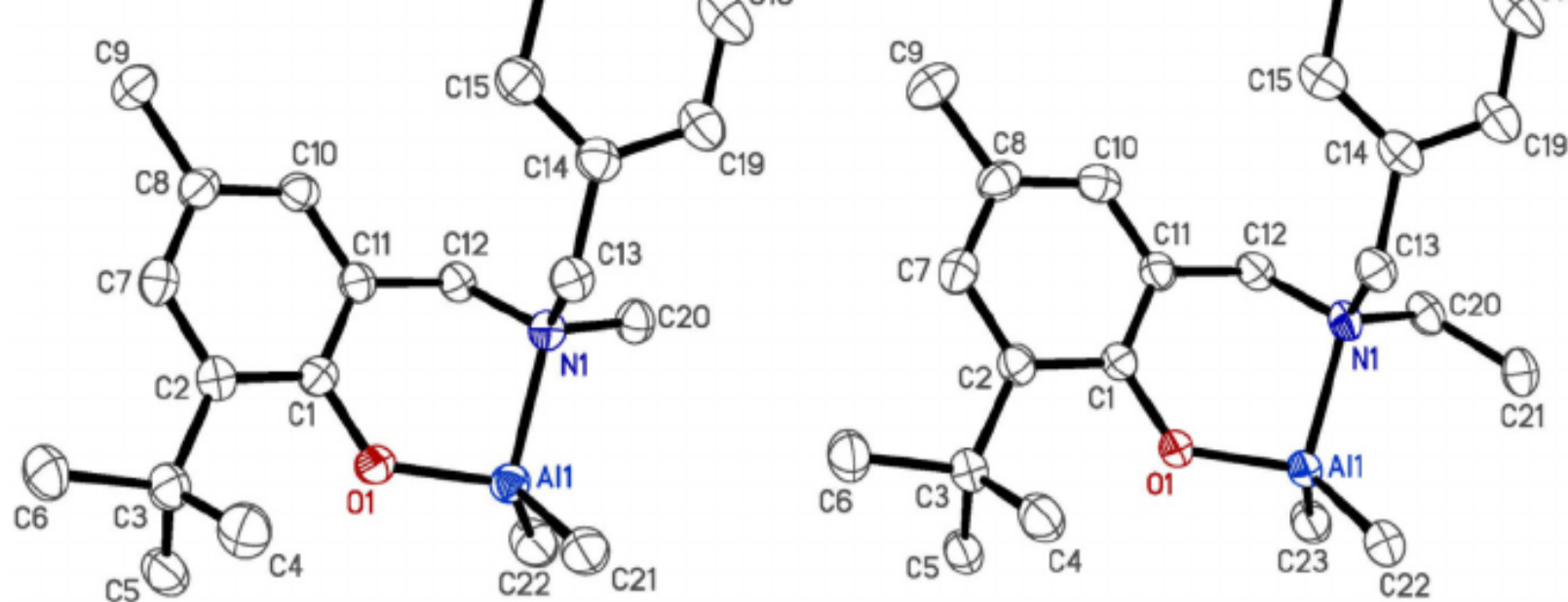
### 2.3.5. Synthesis of L<sup>*p*-Tol</sup>AlMe<sub>2</sub> complex (**2f**)

Complex **2f** was obtained as a white powder, by following a similar procedure to that described for **2a**, from reaction between AlMe<sub>3</sub> (0.34 mL, 0.67 mmol, 2.0 M in hexane) and **1f** (0.24 g, 0.67 mmol). Yield: 0.21 g, 73.0%.  $^1\text{H}$  NMR (400 MHz,  $\text{CDCl}_3$ ):  $\delta$  7.18 (m, 5H, ArH), 7.12–7.04 (m, 3H, ArH), 6.58–6.52 (m, 3H, ArH), 4.52 (d,  $^2J = 14.4$  Hz, 1H, ArCH<sub>2</sub>), 4.39 (d,  $^2J = 13.2$  Hz, ArCH<sub>2</sub>), 4.16 (d,  $^2J = 14.4$  Hz, 1H, ArCH<sub>2</sub>), 3.76 (d,  $^2J = 13.2$  Hz, ArCH<sub>2</sub>), 2.38 (s, 3H, NArCH<sub>3</sub>), 2.27 (s, 3H, ArCH<sub>3</sub>), 1.43 (s, 9H, C(CH<sub>3</sub>)<sub>3</sub>),  $-0.46$  (AlCH<sub>3</sub>),  $-1.26$  (AlCH<sub>3</sub>).  $^{13}\text{C}\{\text{H}\}$  NMR (100 MHz,  $\text{CDCl}_3$ ):  $\delta$  157.0, 143.1, 138.8, 136.7, 131.6, 130.8, 130.4, 128.9, 128.4, 127.9, 125.0, 122.2, 119.5, (all Ar–C), 58.4 (ArCH<sub>2</sub>), 53.2 (PhCH<sub>2</sub>), 35.0 (C(CH<sub>3</sub>)<sub>3</sub>), 29.7 (C(CH<sub>3</sub>)<sub>3</sub>), 21.1 (NArCH<sub>3</sub>), (ArCH<sub>3</sub>),  $-9.5$  (AlCH<sub>3</sub>),  $-10.3$  (AlCH<sub>3</sub>). Anal. Calc. for C<sub>28</sub>H<sub>36</sub>AlNO: C, 78.29%; H, 8.45%; N, 3.26. Found: C, 77.82%; H, 8.94%; N, 3.17%.

### 2.3.6. Synthesis of L<sup>4-ClAr</sup>AlMe<sub>2</sub> complex (**2g**)

Complex **2g** was obtained as a white powder, by following a similar procedure to that described for **2a**, from reaction between AlMe<sub>3</sub> (0.82 mL, 1.63 mmol, 2.0 M in hexane) and **1g** (0.63 g, 1.63 mmol). Yield: 0.63 g, 86.2%.  $^1\text{H}$  NMR ( $\text{CDCl}_3$ , 400 MHz):  $\delta$  7.46–7.38 (m, 1H, ArH), 7.36–7.29 (m, 2H, ArH), 7.27–7.18 (m, 2H, ArH), 7.16–7.07 (m, 3H, ArH), 6.61–6.53 (m, 3H, ArH), 4.57 (d,  $^2J = 14.4$  Hz, 1H, ArCH<sub>2</sub>), 4.39 (d,  $^2J = 12.8$  Hz, 1H, ArCH<sub>2</sub>), 4.20 (d,  $^2J = 14.4$  Hz, 1H, ArCH<sub>2</sub>), 3.79 (d,  $^2J = 12.8$  Hz, 1H, ArCH<sub>2</sub>), 2.28 (s, 3H, ArCH<sub>3</sub>), 1.43 (s, 9H, C(CH<sub>3</sub>)<sub>3</sub>),  $-0.44$  (AlCH<sub>3</sub>),  $-1.23$  (AlCH<sub>3</sub>).  $^{13}\text{C}\{\text{H}\}$  NMR ( $\text{CDCl}_3$ , 100 MHz):  $\delta$  156.9, 144.5, 139.1, 132.8, 130.5, 129.9, 129.8, 129.2, 128.7, 128.2, 125.3, 123.9, 119.2 (all Ar–C), 58.6 (ArCH<sub>2</sub>), 53.7 (ArCH<sub>2</sub>), 35.0 (C(CH<sub>3</sub>)<sub>3</sub>), 29.8 (C(CH<sub>3</sub>)<sub>3</sub>), 21.0 (ArCH<sub>3</sub>),  $-9.5$  (AlCH<sub>3</sub>),  $-10.1$  (AlCH<sub>3</sub>). Anal. Calc. for C<sub>27</sub>H<sub>34</sub>AlNO: C, 78.04%; H, 8.23%; N, 3.37. Found: C, 78.50%; H, 8.71%; N, 3.38%.





*D. Saang'onyo et al./Polyhedron 149 (2018) 153–162*

water, let stir for 5 min and centrifuged for 1 h. Subsequent supernatant was collected (via decantation to exclude insoluble solids) and analyzed by HPLC.

### 2.6. Product analysis

Quantitative analysis of the products was performed by using a Thermo Scientific Dionex Ultimate 3000 HPLC system equipped with a Dionex quaternary pump, a Shodex RI-101 refractive index detector, and a Biorad Aminex HPX-87H column (7.8 mm). 5.0 mM H<sub>2</sub>SO<sub>4</sub> was used as the mobile phase at a rate of 0.6 mL/min, and the column temperature was maintained at 50 °C. The injection volume was 20 μL. All concentrations of glucose, fructose, and HMF in the aqueous phase were determined by comparison to standard calibration curves.

Glucose conversion and products selectivity are defined as follows:

*Glucose conversion* = (moles of glucose reacted)/(initial moles of glucose)

*HMF selectivity* = (moles of HMF produced)/(initial moles of glucose – moles of glucose unreacted)

*HMF yield* = (moles of HMF produced)/(initial moles of glucose)

## 3. Results and discussion

### 3.1. Synthesis and characterization of proligands and complexes

The new (aminomethyl)phenol derivatives **1c–g** (Scheme 1)

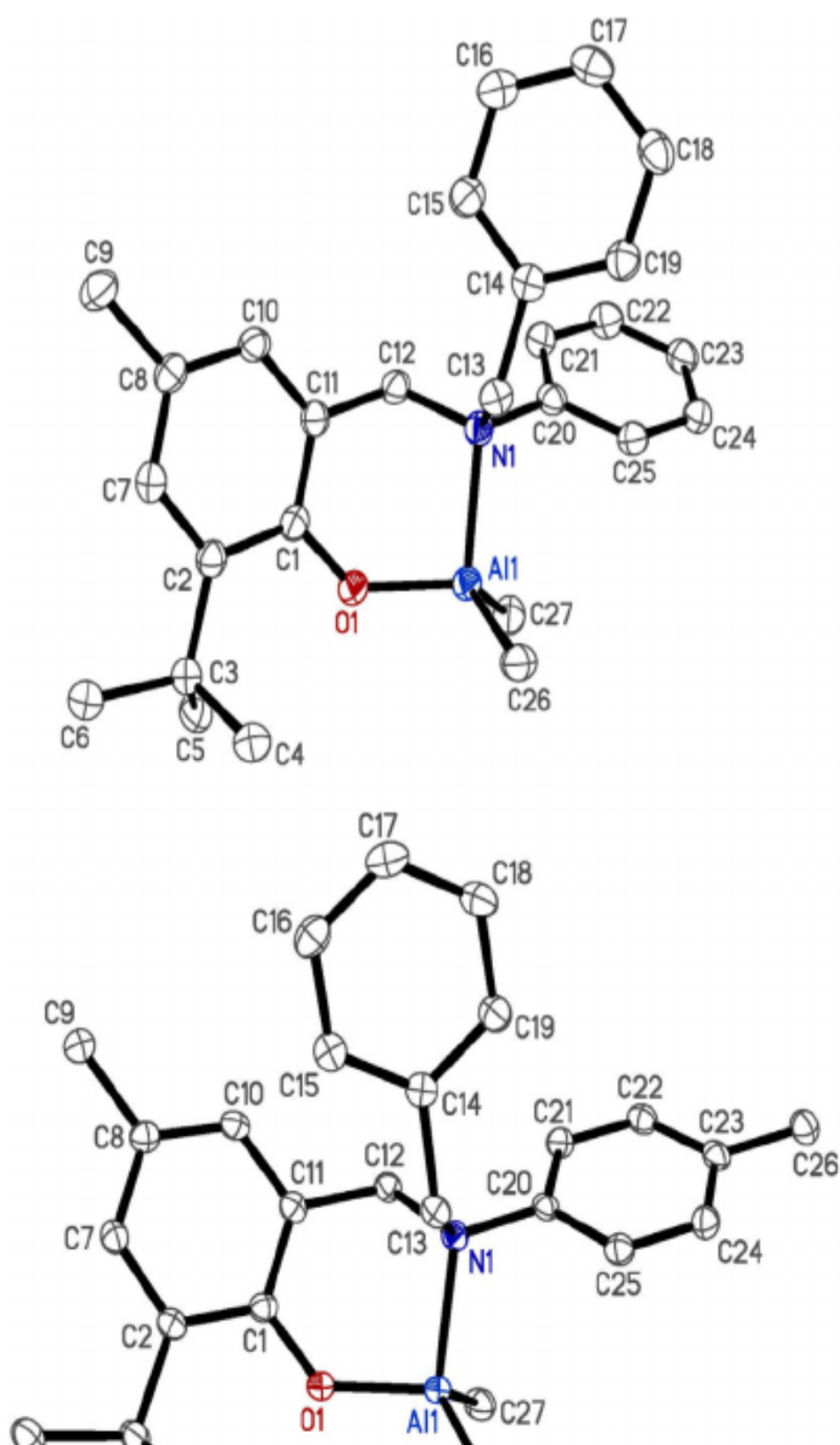




**Fig. 2.** ORTEP diagrams of **2e**, (left) and **2b** (right). Thermal ellipsoids are drawn at 50% probability level. Hydrogens are omitted for clarity.

ALCINO: C, 72.07; H, 7.39; N, 3.11. Found: C, 71.51; H, 7.25; N, 3.08%.

#### 2.4. Crystallographic studies

Single crystals of  $L^RAlMe_2$  complexes **2a–2c** (R = Me, Et, *i*-Pr), **2e** (R = Ph), and **2f** (R = *p*-tolyl) suitable for X-ray crystallographic analysis were obtained by slow recrystallization from a 1:1 *n*-hexane:toluene solution of the complex in the glovebox at room temperature. Colorless single crystals of each complex were placed in dry and degassed paratone oil on a glass plate and used for X-ray diffraction analysis. Crystallographic data for the complexes are collected in Table 1. Further details of the crystallographic study are given in the Supplementary Material.

#### 2.5. General procedure for catalytic dehydration of glucose

All the reactions were performed in a 5-mL reaction vial sealed with a solid cap with PTFE faced silicone septum. In a typical experiment, *D*(+)-glucose (50 mg, 0.28 mmol), [EMIM]Cl (500 mg, 3.41 mmol), and a specified amount of aluminum precatalyst were charged into the reaction vial along with a magnetic stir bar under

were synthesized in good yield by modification of the method reported by Kim and Ishida [27], via neat reaction of 2-*tert*-butyl-4-methylphenol with paraformaldehyde and appropriate catalyst at 105 °C. In addition, compounds **1a** [25] and **1b** [26] were prepared by literature methods.  $L^RAlMe_2$  complexes **2a–g** (Scheme 1) were obtained in good yield via modification of the method reported by Wang and Ma [26] for preparation of  $L^{Et}AlMe_2$  by treatment of proligands **1a–g** with one equivalent of  $AlMe_3$  in toluene at room temperature for 24 h. The reaction proceeded cleanly with evolution of methane to produce **2a–g** which were isolated as moisture-sensitive light-yellow or white powder. The compounds are readily soluble in nonpolar and polar aprotic hydrocarbon solvents, such as chloroform, methylene chloride, diethyl ether, and THF, as well as aromatic hydrocarbon solvents such as benzene and toluene. However, the compounds are only moderately soluble in aliphatic hydrocarbon solvents, and they could be recrystallized from hexane at low temperatures.

The formulation and molecular structure of  $L^RAlMe_2$  complexes **2a** and **2c–g** were established by microanalysis and solution NMR data. Their  $^1H$  NMR spectra did not show the downfield resonance characteristic of the phenolic OH group of the proligands, supporting coordination of phenolate oxygen with aluminum. Contrary to the bidentate coordination of the (aminomethyl)phenol ligand, with tight binding of the amino nitrogen to aluminum, resulting in hindered rotation of *N*-benzyl group on the NMR time scale at room temperature, the  $^1H$  NMR spectra of  $L^RAlMe_2$  complexes **2a** and **2c–g** contained four doublet resonances in the 4.57–3.55 ppm range for the four benzylic protons. Similarly, chemically inequivalent methyl resonances were observed for the *N*-isopropyl group of **2c**, consistent with coordination of

2e		2f	
589(8)	Al(1)–O(1)	1.7616(9)	Al(1)–O(1)
619(11)	Al(1)–C(27)	1.9570(14)	Al(1)–C(28)
647(11)	Al(1)–C(26)	1.9638(13)	Al(1)–C(27)
727(9)	Al(1)–N(1)	2.0532(10)	Al(1)–N(1)
0.95(4)	O(1)–Al(1)–C(27)	110.42(5)	O(1)–Al(1)–C(28)
3.86(4)	O(1)–Al(1)–C(26)	113.27(5)	O(1)–Al(1)–C(27)
3.74(5)	C(27)–Al(1)–C(26)	118.92(6)	C(28)–Al(1)–C(27)
36(3)	O(1)–Al(1)–N(1)	94.95(4)	O(1)–Al(1)–N(1)
0.30(4)	C(27)–Al(1)–N(1)	110.52(5)	C(28)–Al(1)–N(1)
5.45(4)	C(26)–Al(1)–N(1)	105.97(5)	C(27)–Al(1)–N(1)
..59(7)	C(20)–N(1)–Al(1)	109.24(7)	C(20)–N(1)–Al(1)

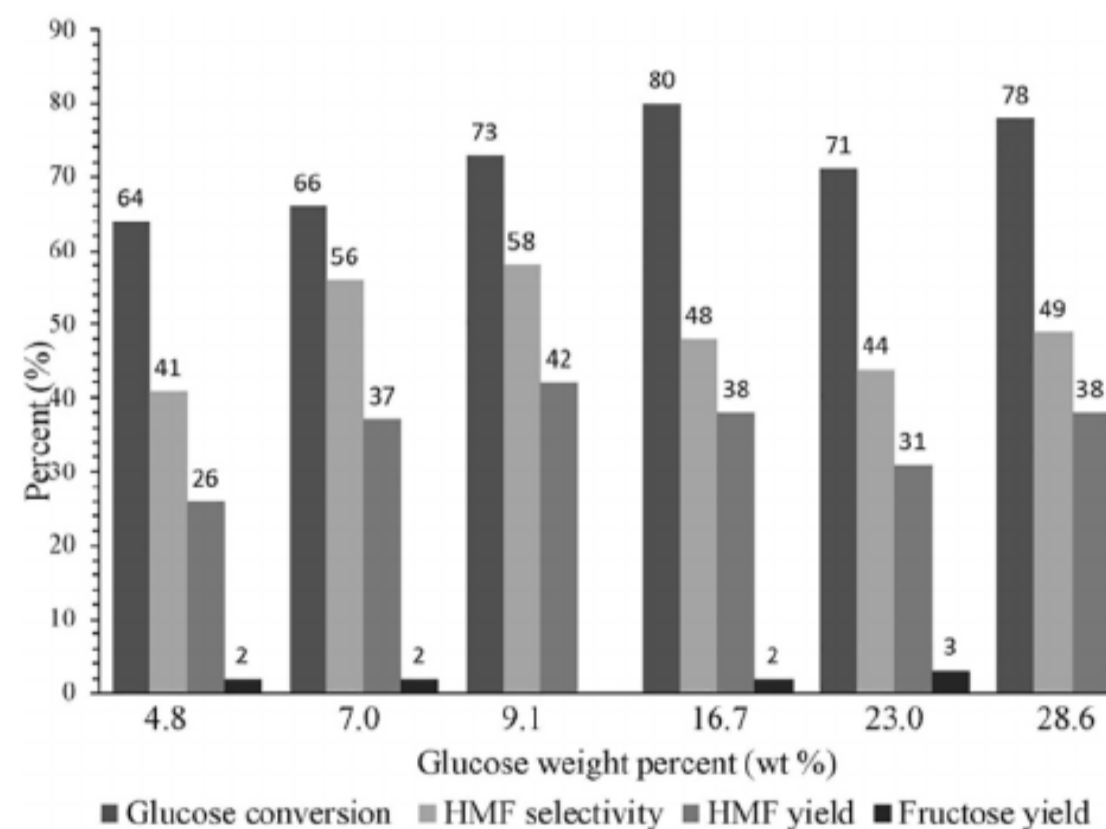


**Fig. 3.** The effect of glucose weight percent in [EMIM]Cl on the product distribution. Reaction conditions: 50 mg glucose using 5 mol% [ $L^{Ph}AlMe_2$ ] (0.14 mmol) in [EMIM]Cl (500 mg, 3.41 mmol) at 120° C for 2 h.

$C_1$  symmetry expected for tetrahedral  $L^RAlMe_2$  complexes **2a–g**, two different Al–CH<sub>3</sub> resonances were observed in their  $^1H$  NMR spectra in the upfield region of –0.56 to –0.86 ppm for complexes **2a–2d** (with *N*-alkyl substituent), and –0.43 to –1.26 ppm for **2e–g** (with *N*-aryl substituent).  $^{13}C\{^1H\}$  NMR spectra of these complexes are also consistent with their  $C_1$  symmetry; together with two Al–CH<sub>3</sub> and two benzylic carbon resonances, **2a, 2c, and 2d** each displayed ten aromatic carbon resonances while **2b, 2e, and 2f** each displayed fourteen aromatic carbon resonances.

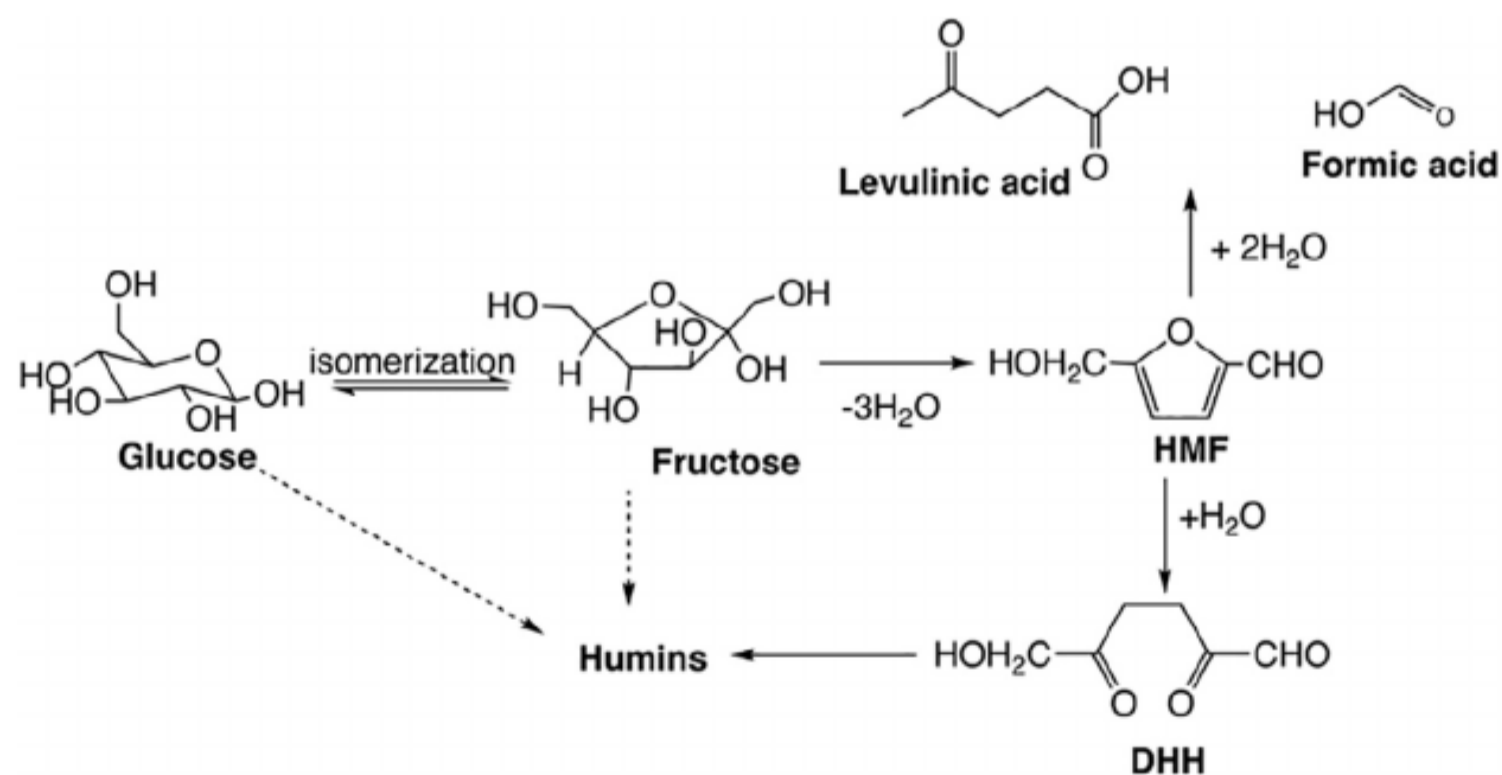
l lengths (Å) and bond angles (°) for L<sup>Ph</sup>AlMe<sub>2</sub> complexes **2a–2c**, **2e**, and **2f**.

	<b>2b</b>	<b>2c</b>
Al(1)–O(1)	1.7559(10)	1.7474(16)
Al(1)–C(22)	1.9470(16)	1.965(3)
Al(1)–C(23)	1.9542(16)	1.966(3)
Al(1)–N(1)	2.0284(12)	2.027(2)
O(1)–Al(1)–C(22)	111.53(7)	109.99(10)
O(1)–Al(1)–C(23)	111.66(6)	110.45(10)
C(22)–Al(1)–C(23)	117.33(8)	119.21(12)
O(1)–Al(1)–N(1)	96.53(5)	97.17(8)
C(22)–Al(1)–N(1)	108.36(6)	110.44(10)
C(23)–Al(1)–N(1)	109.35(6)	107.31(10)
C(20)–N(1)–Al(1)	109.58(8)	109.88(15)

X-ray diffraction analysis on single-crystals of **2a–2c**, **2e**, and **2f** confirmed the structure assigned by spectroscopy. Structures of the complexes are depicted in Figs. 1 and 2, and crystallographic data and selected metrical parameters for the complexes are collected in Tables 1 and 2. The compounds adopt a distorted tetrahedral structure with the (aminomethyl)phenolate ligand coordinated to aluminum in bidentate fashion, via phenolate oxygen and amino nitrogen atoms. The aluminum center is also coordinated by two carbon atoms from two methyl groups. The distortion from idealized tetrahedral geometry arises from the acute bite angle of the chelating (aminomethyl)phenolate ligand [O(1)–Al(1)–N(1) bond angles range from ca. 95° to 97°], which is compensated for by opening of the C–Al–C, C–Al–O, and C–Al–N bond angles (Table 2). All of the Al–O, Al–N and Al–C bond distances are within the range reported for related complexes [28–30]. However, **2a** and **2b** (with NMe(CH<sub>2</sub>Ph) or NMe(*i*-Pr)(CH<sub>2</sub>Ph) moiety, respectively) possessed shorter Al–N bond distances (<2.03 Å) than were observed (>2.05 Å, Table 2) for **2c** (with N(*i*-Pr)(CH<sub>2</sub>Ph) moiety), **2e** (with NPh(CH<sub>2</sub>Ph) moiety) or **2f** (with N(*p*-MeC<sub>6</sub>H<sub>4</sub>)(CH<sub>2</sub>Ph) moiety). Presumably, this is because electron-releasing methyl and ethyl substituents increase electron donation by amino nitrogen atom to aluminum, relative to bulkier isopropyl substituent or less electron donating aryl substituents. The molecular structures (Figs. 1 and 2) confirmed that in **2e** and **2f** the two Al–CH<sub>3</sub> groups reside in a more dissimilar chemical environment than in **2a–c**, consistent with <sup>1</sup>H NMR data (vide supra). In **2e** and **2f**, one Al–Me group lies in close proximity to the *N*-aryl ring; for **2e**, the torsion angle between Al–Me and phenyl ring (C27–Al(1)–N1–C20) is 27.52° and the C20–C27 distance is 3.297 Å.

### 3.2. Glucose dehydration studies

D. Saang'onyo et al./Polyhedron 149 (2018) 153–162



Scheme 2. Possible pathways for glucose conversion to HMF and other products.

sion and the product distribution of glucose dehydration at 120 °C for 2 h using 5 mol% (relative to moles of glucose) L<sup>Ph</sup>AlMe<sub>2</sub> (**2e**) as catalyst. The glucose conversion ranged between 73% and 80% for glucose concentrations in [EMIM]Cl ranging between 9.1 and 28.6 wt%. However, the highest HMF selectivity and yield (58% and 42%, respectively) were both obtained when 9.1 wt% glucose was employed. It is known that Lewis acid-catalyzed glucose dehy-

#### 3.2.2. Effect of temperature and time

Table 3 shows the effects of temperature and time on glucose dehydration in [EMIM]Cl using [L<sup>Ph</sup>AlMe<sub>2</sub>] (**2e**, 5 mol%) as catalyst. The reaction was investigated in the absence and presence of catalyst over the 100–140 °C temperature range. At all temperatures in the absence of a catalyst, both the glucose conversion (3%) and the HMF yield (<1%) were quite poor, consistent with pr

dration generally proceeds via glucose isomerization to fructose, followed by fructose dehydration to HMF (Scheme 2) [6]. Predictably, all of the product mixtures also contained a small amount of fructose (2–3%) except for when 9.1 wt% glucose in [EMIM]Cl was employed, whereupon fructose was present only in trace amount. No other soluble products were detected by HPLC analysis in the supernatants obtained after aqueous extraction of any of the dark brown reaction mixtures; these results and all other results reported herein were reproduced at least 3 times. Since glucose concentrations  $\geq 9.1$  wt% resulted in comparable conversions while both the HMF selectivity and HMF yield decreased when  $>9.1$  wt% glucose in [EMIM]Cl was employed, all other experiments reported herein were conducted using 9.1 wt% sugar in ionic liquid solvent, unless otherwise indicated.

literature reports.[11,31] For example, Zhao et al. reported 40% glucose conversion and <4% HMF yield when 9.1 wt% glucose in [EMIM]Cl was heated at 180 °C for 3 h in the absence of a catalyst.[11] In the presence of [L<sup>Ph</sup>AlMe<sub>2</sub>] (**2e**), the conversion of glucose at 100 °C increased gradually with time, reaching a maximum of 59% after 6 h (Table 3, entries 3–6). The HMF selectivity increased up to 56% over four hours of reaction, and remained at 56% after 6 h, resulting in 33% HMF yield. As expected, glucose conversion increased with an increase in temperature. Consequently, 95% glucose conversion was achieved at 120 °C after 6 h. However, as the data in Table 3 (entries 11–14) show, glucose conversion slowed dramatically as the reaction progressed, with only a slight increase in glucose conversion observed after 4 h. While this reflects the reduction in reaction rate as the concentration of

**Table 3**

Temperature and time effects on glucose dehydration in [EMIM]Cl in absence and presence of a catalyst. <sup>a</sup>

Entry	Temp (°C)	Time (min)	Cat. <sup>b</sup>	Glucose Conv. (%)	HMF selectivity (%)
1	100	1	–	3	0
2	100	2	–	4	0
3	100	1	<b>2e</b>	17	38
4	100	2	<b>2e</b>	31	43
5	100	4	<b>2e</b>	46	56
6	100	6	<b>2e</b>	59	56
7	120	1	–	4	0
8	120	2	–	6	0
9	120	4	–	8	5
10	120	6	–	15	5
11	120	1	<b>2e</b>	52	53
12	120	2	<b>2e</b>	69	54
13	120	4	<b>2e</b>	88	53
14	120	6	<b>2e</b>	95	49
15	140	1	–	23	<1
16	140	0.33 <sup>c</sup>	<b>2e</b>	70	47
17	140	0.66 <sup>d</sup>	<b>2e</b>	85	45
18	140	1	<b>2e</b>	92	48

**Table 4**

The effect of catalyst ([L<sup>Ph</sup>AlMe<sub>2</sub>], **2e**) loading on glucose dehydration in [EMIM]Cl. <sup>a</sup>

Entry	Temp (°C)	Catalyst mol%	Glucose conv. (%)	HMF selectivity (%)	HMF yield (%)
<b>1</b>	100	5	46	56	26
<b>2</b>	100	10	65	42	27
<b>3</b>	100	15	69	43	30
<b>4</b>	100	20	71	39	28
<b>5</b>	120	5	88	53	46
<b>6</b>	120	10	94	45	42
<b>7</b>	120	15	95	45	43
<b>8</b>	120	20	97	42	40

<sup>a</sup> Reaction conditions: 9.1 wt% glucose at the indicated temperature for 4 h.

glucose decreases, it is noteworthy that the HMF selectivity remained more or less constant (53–54%) over 4 h, and decreased only slightly (to 49%) after 6 h. This result argues against significant catalyst deactivation occurring during the reaction since the HMF selectivity remained essentially constant as the glucose conversion increased. Accordingly, the HMF yield increased up to 46% after 4 h and was essentially unchanged after 6 h.

Raising the reaction temperature to 140 °C resulted in 92% glucose conversion after 1 h, along with 48% HMF selectivity and 44%

increase in the catalyst loading resulted in unchanged or slightly decreased HMF selectivity and yield. Thus, it appears that catalyst loadings higher than 5 mol% enhance side reactions that lead to the formation of humins (*vide infra*).

### 3.2.4. Ligand effects

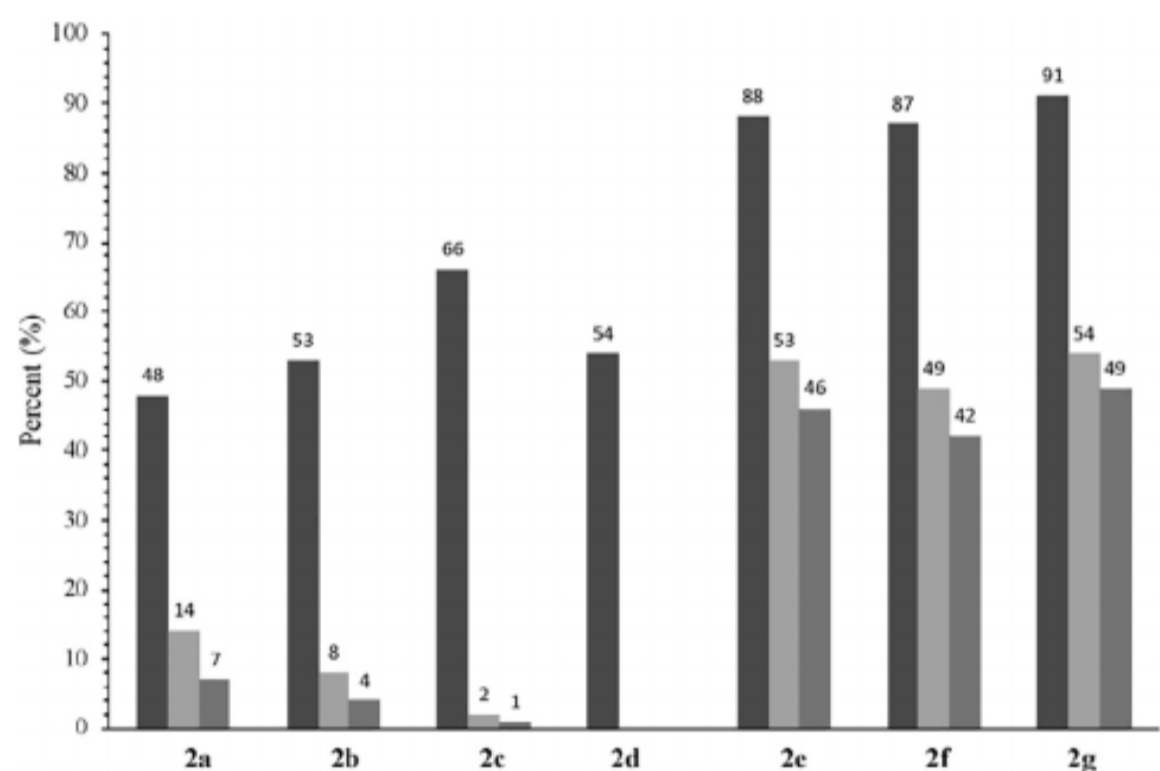
The potential of L<sup>R</sup>AlMe<sub>2</sub> complexes **2a–g** as catalysts for glucose dehydration to HMF was investigated by conducting the reaction in [EMIM]Cl at 120 °C for 4 h using 5 mol% of **2a–g** as catalyst.



HMF yield. Consequently, we investigated the effect of shorter reaction time for  $[L^{Ph}AlMe_2]$  (**2e**)-catalyzed glucose conversion at 140 °C (Table 3, entries 16 and 17). 70% glucose conversion was observed after 20 min but the reaction progress slowed dramatically once again, with only 15% additional glucose conversion observed after another 20 min of reaction. However, while glucose conversion increased on raising the reaction temperature from 120 to 140 °C, the HMF selectivity and hence the HMF yield decreased slightly although shorter time was required to reach high conversion (Table 3).

### 3.2.3. Effect of catalyst loading

Table 4 shows results of our study of the effect of catalyst loading on glucose conversion and the product distribution for  $[L^{Ph}AlMe_2]$  (**2e**)-catalyzed dehydration of glucose in [EMIM]Cl at both 100 and 120 °C for 4 h; the catalyst loading was varied in 5% increments from 5 to 20 mol%. At both temperatures, a modest increase in glucose conversion accompanied an increase in the catalyst loading from 5 to 10 mol% while further increase in the catalyst loading had little effect on the extent of reaction. Conversely, both the HMF selectivity and yield decreased significantly upon increasing the catalyst loading from 5 to 10 mol% while further



As shown by the glucose conversion and product distribution in Fig. 4,  $L^RAlMe_2$  complexes **2a-d** for which the R substituent is an alkyl group (Scheme 1) were ineffective catalysts for selective formation of HMF. The glucose conversion was modest (~5% even if significantly higher than in absence of a catalyst (Table 3, entry 9). But more importantly, both the HMF selectivity and yield were extremely poor. The HMF yield in fact decreased as size of amino moiety's alkyl substituent increased, with only a trace amount of HMF produced when **2d** ( $L^RAlMe_2$ , R = Bu<sup>t</sup>) was used as catalyst.

The difference in catalytic efficiency of  $L^RAlMe_2$  complexes containing alkyl-substituted amino group (**2a-d**) versus aryl-substituted amino group (**2e-g**) is remarkable. All of the aryl-substituted aluminum (aminomethyl)phenolate complexes **2e-g** afforded much higher glucose conversion (>87%) and much better HMF selectivity (49–54%) and yield (42–49%) than alkyl-substituted aluminum (aminomethyl)phenolate complexes **2a-d** (Fig. 4). As the data in Table 2 show, bond angles about the Al and N atoms are similar for all of the complexes. However, Al–N bond distances for **2a** and **2b** are significantly shorter than those for **2e** and **2f**, due presumably to stronger sigma electron donation to aluminum by alkyl-substituted nitrogen relative to aryl-substituted nitrogen. On the other hand, the significantly longer Al–O bond distance for **2c** (compared to **2a** and **2b**) is most probably due to its sterically more crowded coordination sphere. Thus, we presume that the markedly decreased efficiency of **2a-d** as glucose dehydration catalysts (versus **2e-g**) is due to the reduced Lewis acidity of **2a-d**, and/or greater steric hindrance at the aluminum center in complexes **2c** and **2d**. In this regard, a slight increase in both the HMF selectivity and yield was observed as electron donation from aryl-substituted amino group was decreased by decreasing the electron releasing ability of the para substituent of the amino group (Fig. 4), that is, from R = *p*-MeC<sub>6</sub>H<sub>4</sub> (**2f**) to R = C<sub>6</sub>H<sub>5</sub> (**2e**) to R = *p*-ClC<sub>6</sub>H<sub>4</sub> (**2g**) [32]. Clearly, the different (aminomethyl)phenolate ligands impose different chemical (coordination) environments about the Al center, consistent with the different chemical shifts observed for the Al–Me groups of **2a-d** versus **2e-g** (Section 3.1).

D. Saang'onyo et al./Polyhedron 149 (2018) 153–162

**Table 5**

Ionic liquid effects on glucose dehydration with  $[L^{Ph}AlMe_2]$  (**2e**) as catalyst.

Entry	Ionic liquid (IL)	Time (h)	Glucose conv. (%)	HMF selectivity (%)
<b>1<sup>a</sup></b>	[EMIM]Br	1	56	56
<b>2<sup>a</sup></b>	[EMIM]Br	2	74	59
<b>3<sup>a</sup></b>	[EMIM]Br	4	84	64
<b>4<sup>a</sup></b>	[EMIM]Br	6	91	55
<b>5<sup>a</sup></b>	[BMIM]Br	1	92	56
<b>6<sup>a</sup></b>	[BMIM]Br	2	97	60
<b>7<sup>a</sup></b>	[BMIM]Br	4	100	55
<b>8<sup>b</sup></b>	[BMIM]Br	2	95	63

<sup>a</sup> Reaction conditions: 9.1 wt% glucose with 5 mol%  $[L^{Ph}AlMe_2]$  (**2e**) at 120 °C.

<sup>b</sup> 4.8 wt% glucose and 5 mol%  $[L^{Ph}AlMe_2]$  (**2e**) at 120 °C.

during dehydration of sugars [9,35,36]. In this regard, Lunelli et al. [37,38] have proposed a mechanism for humin formation in the presence of 2,5-dioxo-6-hydroxyhexanal (DHH), formed by HMF rehydration. DHH is a key intermediate (Scheme 2). Humins were proposed

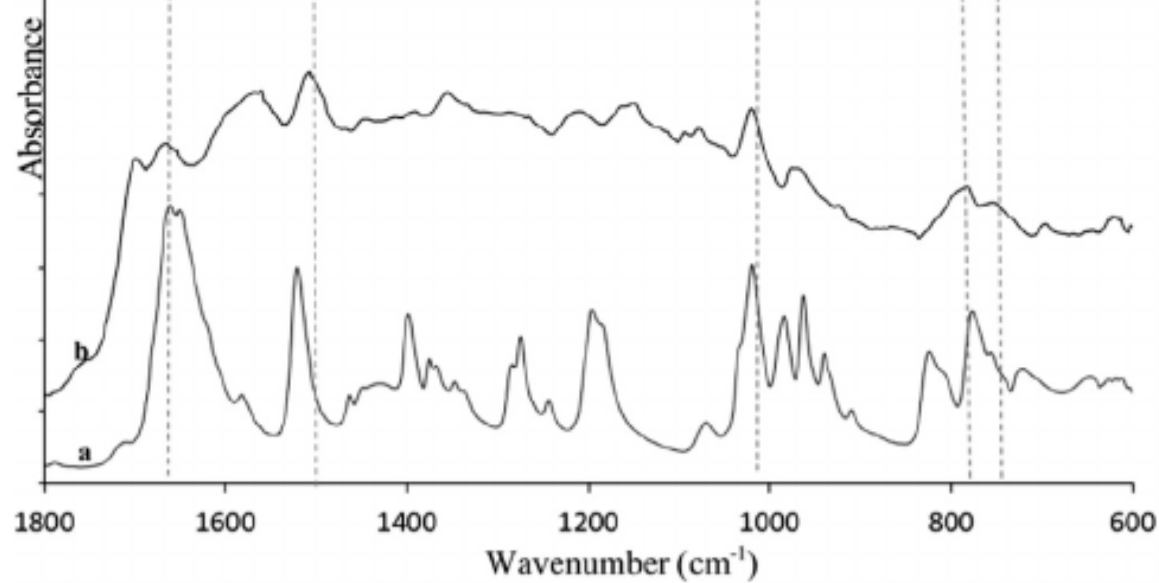


**Fig. 5.** ATR-IR spectra of (a) HMF and (b) humins formed during  $L^{\text{Ph}}\text{AlMe}_2$  (**2e**)-catalyzed glucose dehydration in [EMIM]Cl at 120 °C for 4 h.

as in [EMIM]Cl (Table 3, entries 11–14), the HMF selectivity and yield were significantly higher in [EMIM]Br, peaking after 4 h at 64% and 54%, respectively. Higher HMF selectivity and yield have previously been observed in the presence of bromide ion relative to chloride ion, and have been attributed to acceleration of fructose dehydration as a result of better nucleophilicity and leaving group properties of bromide ion [33,34]. As mentioned earlier, fructose is the only other soluble product observed in our reactions, and Lewis acid-catalyzed glucose dehydration generally occurs via glucose isomerization to fructose [6].

Glucose conversion progressed significantly faster in [BMIM]Br (1-butyl-3-methylimidazolium bromide) than in [EMIM]Br, reaching 92% in 1 h, and giving HMF selectivity and yield of 56% and 52%, respectively. Increasing the reaction time to 2 h resulted in slightly higher glucose conversion and an increase in the HMF selectivity and yield to 60% and 58%, respectively. However, further increase in the reaction time resulted in a decrease in the HMF selectivity and yield (Table 5, entry 7). Since glucose conversion was much faster in [BMIM]Br, we investigated the effect of lowering the concentration of glucose in [BMIM]Br from 9.1 wt% to 4.8 wt% on the HMF selectivity and yield: 95% glucose conversion was achieved after 2 h, along with slight increases in the HMF selectivity and yield, up to 63% and 60%, respectively (Table 5, entry 8).

### 3.3. Humins analysis

incorporation of HMF in their structure, the HMF selectivity of  $L^{\text{R}}\text{AlMe}_2$ -catalyzed glucose dehydration appears to be limited by competing loss of HMF to humins formation.

The reasonably high yield of HMF (60%) obtained herein from  $L^{\text{Ph}}\text{AlMe}_2$ -catalyzed glucose dehydration in ionic liquids is encouraging, as is our finding that the catalytic efficiency of  $L^{\text{R}}\text{AlMe}_2$  complexes can be tuned via modification of the (aminomethyl)phenolate ligand. To date, the vast majority of studies of aluminum-catalyzed glucose conversion to HMF have focused on  $\text{AlCl}_3$ . The findings from this study are useful toward developing better understanding of the relationship between the structure and function of aluminum catalysts for glucose (and ultimately cellulose) conversion into HMF. Towards this end, we have recently initiated a study of the reactions of  $L^{\text{Me}}\text{AlMe}_2$  (**2a**) and  $L^{\text{Ph}}\text{AlMe}_2$  (**2e**) with glucose and cycloalkane diols in ionic liquid solvents.

### Acknowledgements

formed via subsequent aldol condensations of DHH with the carbonyl group of HMF, with the extent of HMF incorporation into the humin structure being dependent on the accumulation of HMF during the reaction. Furthermore, it was suggested that humins could not be directly formed from sugars. Zandvoort et al. [37] have similarly suggested that humins are mainly derived from HMF based on their finding that addition of HMF to the glucose feed barely changed the elemental composition of the humins obtained from acid-catalyzed dehydration of glucose. HPLC analysis of the product mixtures from glucose and fructose dehydration catalyzed with aluminum (aminomethyl)phenolate complex (**2g**) detected HMF as well as glucose and/or fructose as the only products. Thus, formation of humins rather than HMF rehydration to form levulinic acid (LA) and formic acid (FA) appears to be the main route for HMF loss in these reactions (Scheme 2).

The nature of the insoluble brown solids produced during  $L^{\text{R}}\text{AlMe}_2$  (**2e**)-catalyzed dehydration of glucose (for 4 h) in [EMIM]Cl at 120 °C was investigated by Raman and ATR-FTIR spectroscopy. The Raman data are suggestive of the presence of aromatic groups with oxygen-rich functionalities. The signals at 1385 and 1585  $\text{cm}^{-1}$  are characteristic of the D and G bands of ordered graphite-like carbon [37,39,40]. Fig. 5 compares ATR-IR spectra of the humins with the IR spectrum of HMF. The humin spectra show broad absorbance peaks in ca. 1100–1400  $\text{cm}^{-1}$  range with peaks that arise from the furan ring of HMF [37,41]. Specifically, the two peaks in the 750–850  $\text{cm}^{-1}$  range, the peak at 1020  $\text{cm}^{-1}$ , and the peak at 1512  $\text{cm}^{-1}$  have been attributed to the furan ring of HMF. These data strongly support significant incorporation of HMF into the humin structure.

### 4. Conclusions

$L^{\text{R}}\text{AlMe}_2$  complexes **2e–g**, which contain a bidentate (aminomethyl)phenolate ligand with an aryl substituent on the phenolate group, are efficient catalysts for glucose dehydration in ionic liquid solvents to give HMF. In [EMIM]Br and [BMIM]Br, the reaction proceeds at 120 °C with very high conversion in 2 h to produce HMF with 60–63% selectivity and in 58–60% yield. Both the HMF selectivity and yield were lower in [EMIM]Cl, up to 54% and 49%, respectively. The HMF selectivity of glucose dehydration decreased as the concentration of the aluminum catalyst was increased from 20 mol%. Giving that no other soluble products (besides gl

- [2] C.B. Rasrendra, I.G.B.N. Makertihartha, S. Adisasmito, H.J. Heeres, *Top. Catal.* (2010) 1241.
- [3] B.R. Caes, R.E. Teixeira, K.G. Knapp, R.T. Raines, *ACS Sustainable Chem. Eng.* (2015) 2591.
- [4] H. Li, F. Chang, Y. Zhang, D. Hu, L. Jin, B. Song, S. Yang, *Curr. Catal.* 1 (2012).
- [5] R.-J. van Putten, J.C. van der Waal, E. de Jong, C.B. Rasrendra, H.J. Heeres, J. Vries, *Chem. Rev.* (Washington, DC, U. S.) 113 (2013) 1499.
- [6] A. Corma, S. Iborra, A. Velty, *Chem. Rev.* (Washington, DC, U. S.) 107 (2008) 2411.
- [7] M. Bicker, J. Hirth, H. Vogel, *Green Chem.* 5 (2003) 280–284.
- [8] G.W. Huber, S. Iborra, A. Corma, *Chem. Rev.* (Washington, DC, U. S.) 106 (2006) 4044.
- [9] J.-P. Lange, R. Price, P.M. Ayoub, J. Louis, L. Petrus, L. Clarke, H. Gosse, *Angew. Chem. Int. Ed.* 49 (2010) 4479.
- [10] Y.J. Pagan-Torres, T. Wang, J.M.R. Gallo, B.H. Shanks, J.A. Dumesic, *ACS Catal.* (2012) 930.
- [11] H. Zhao, J.E. Holladay, H. Brown, Z.C. Zhang, *Science* (Washington, DC, U.S.) (2007) 1597.
- [12] Y. Zhang, E.A. Pidko, E.J.M. Hensen, *Chem. Eur. J.* 17 (2011) 5281.
- [13] J.B. Binder, R.T. Raines, *J. Am. Chem. Soc.* 131 (2009) 1979.
- [14] S. Hu, Z. Zhang, J. Song, Y. Zhou, B. Han, *Green Chem.* 11 (2009) 1746.
- [15] K.R. Enslow, A.T. Bell, *Catal. Sci. Technol.* 5 (2015) 2839.

We are grateful to the Kentucky Science Foundation (grant number KSEF-2428-RDE-014) for partial financial support of this work. We are also grateful to US National Science Foundation (grant number CBET 1604491) for partial financial support of this research. NMR instruments utilized in this research were funded in part by the CRIF program of the US National Science Foundation (grant number CHE-9974810). The X8 Proteum and D8 Venture diffractometers were funded by the NSF (MRI CHE0319176 and CHE1625732 respectively). The authors are also grateful to Professor Darrin L. Smith (Chemistry Department, Eastern Kentucky University) for generously providing access and helping with HPLC analysis. DS is grateful to Professor Anne-Frances Miller and Mr. John Layton for helpful advice with regard to NMR.

### Appendix A. Supplementary data

CCDC 1489633, 1489630, 1812487, 1489632, and 1489631 contains the supplementary crystallographic data for complexes **2a–c**, **2e** and **2f**, respectively. These data can be obtained free of charge via <http://www.ccdc.cam.ac.uk/conts/retrieving.html>, or from the Cambridge Crystallographic Data Centre, 12 Union Road, Cambridge CB2 1EZ, UK; fax: (+44) 1223-336-033; or e-mail: [deposit@ccdc.cam.ac.uk](mailto:deposit@ccdc.cam.ac.uk). Supplementary data associated with this article can be found, in the online version, at <https://doi.org/10.1016/j.poly.2018.03.035>.

### References

- [1] A. Chinnappan, C. Baskar, H. Kim, *RSC Adv.* 6 (2016) 63991.

- [16] Y. Yang, C. Hu, M.M. Abu-Omar, *Bioresour. Technol.* 116 (2012) 190.  
[17] Y. Yang, C. Hu, M.M. Abu-Omar, *J. Mol. Catal. A: Chem.* 376 (2013) 98.  
[18] X. Zhang, P. Murria, Y. Jiang, W. Xiao, H.I. Kenttamaa, M.M. Abu-Omar, Mosier, *Green Chem.* 18 (2016) 5219.  
[19] C. Rasrendra, J. Soetedjo, I. Makertihartha, S. Adisasmito, H. Heeres, *Top. Catal.* 55 (2012) 543.  
[20] D. Liu, E.Y.X. Chen, *Appl. Catal. A* 435–436 (2012) 78.  
[21] W.L.F. Armarego, D.D. Perrin, *Purification of Laboratory Chemicals*, Fourth Edition, Butterworths, London, 1997.  
[22] P. Nockemann, K. Binnemans, K. Driesen, *Chem. Phys. Lett.* 415 (2005) 1.  
[23] P.N. Tshibangu, S.N. Ndwandwe, E.D. Dikio, *Int. J. Electrochem. Sci.* 6 (2011) 2201.  
[24] S. Enthaler, *Catal. Lett.* 141 (2011) 55.  
[25] J.-B. Cazaux, P. Braunstein, L. Magna, L. Saussine, H. Olivier-Bourbigou, *Eur. J. Inorg. Chem.* (2009) 2942.  
[26] Y. Wang, H. Ma, *J. Organomet. Chem.* 731 (2013) 23.  
[27] H.-D. Kim, H. Ishida, *J. Phys. Chem. A* 106 (2002) 3271.  
[28] L. Chen, W. Li, D. Yuan, Y. Zhang, Q. Shen, Y. Yao, *Inorg. Chem.* 54 (2015) 4.  
[29] A. Maise-Francois, L. Azor, A.-L. Schmitt, A. Coquel, L. Brelot, R. Welt, Bellemin-Laponnaz, S. Dagorne, *J. Organomet. Chem.* 696 (2012) 4248.  
[30] S. Dagorne, *J. Organomet. Chem.* 691 (2006) 4797.  
[31] W. Liu, J. Holladay, *Catal. Today* 200 (2013) 106.  
[32] M.B. Smith, J. March, *March's Advanced Organic Chemistry: Reaction Mechanisms, and Structure*, 5th ed., 2000.  
[33] P. Wrigstedt, J. Keskivaali, M. Leskelae, T. Repo, *ChemCatChem* 7 (2015) 1.  
[34] Y. Yang, W. Liu, N. Wang, H. Wang, W. Li, Z. Song, *Chin. J. Chem.* 33 (2015) 1.  
[35] B. Girisuta, L.P.B.M. Janssen, H.J. Heeres, *Ind. Eng. Chem. Res.* 46 (2007) 1.  
[36] J. Horvat, B. Klaić, B. Metelko, V. Sunjic, *Tetrahedron Lett.* 26 (1985) 211.  
[37] S.K.R. Patil, J. Heltzel, C.R.F. Lund, *Energy Fuels* 26 (2012) 5281.  
[38] S.K.R. Patil, C.R.F. Lund, *Energy Fuels* 25 (2011) 4745.  
[39] I. van Zandvoort, Y. Wang, C.B. Rasrendra, E.R.H. van Eck, P.C.A. Bruijninx, Heeres, B.M. Weckhuysen, *ChemSusChem* 6 (2013) 1745.  
[40] C. Yao, Y. Shin, L.-Q. Wang, C.F. Windisch Jr., W.D. Samuels, B.W. Arey, C. W. W.M. Risen Jr., G.J. Exarhos, *J. Phys. Chem. C* 111 (2007) 15141.  
[41] Y.-S. Lim, H.-S. Kim, M.-S. Kim, N.-H. Cho, S. Nahm, *Macromol. Res.* 11 (2002) 122.